Proceedings of Ninth World Conference on Earthquake Engineering
August 2-9, 1988, Tokyo-Kyoto, JAPAN (Vol.VI)

10-2-11

DYNAMIC RESPONSE ANALYSIS OF A FIVE-SPAN CONTINUOUS RIGID-FRAME BRIDGE WITH V-SHAPED LEGS

Toshiro HAYASHIKAWA[1], Takakichi KANEKO[2], Yoshitaka MATSUI[3], and Koichi YOSHIDA[4]

[1]Department of Civil Engineering, Hokkaido University, Kita-ku, Sapporo, Japan
[2]Department of Civil Engineering, Senshu University Hokkaido College, Bibai, Japan
[3]Chuoh Consultants Co., Ltd., Kita-ku, Sapporo, Japan
[4]Research Institute of Hokkaido Development Bureau, Toyohira-ku, Sapporo, Japan

SUMMARY

Dynamic response analysis is performed of a five-span continuous rigid-frame steel bridge with V-shaped legs standing on two reinforced concrete piers. Three different analytical matrix methods for determining the dynamic characteristics of in-plane vibrating rigid-frame bridges are presented. The numerical results computed by using the lumped, consistent, and continuous mass methods are given in tabular form, and their accuracy is evaluated. Also, the Square-Root-of-Sum-of-Squares (SRSS) method and the Complete Quadratic Combination (CQC) method are used for seismic analyses that combines modal maxima. The calculation results are compared with those resulting from a time history response analysis.

INTRODUCTION

Over the last three decades significant research has been conducted in the field of earthquake engineering to better understand the performance of structures during strong earthquakes. Numerous rigid-frame bridges have been designed recently for use as highway bridges in earthquake-prone areas. It is thus important to take into account the structurally complex superstructures that characterize rigid-frame bridges with V-shaped legs. Because of the long spans typically involved, their superstructures are relatively flexible both vertically and transversely. The seismic response of rigid-frame bridge structures is usually dominated by both lower and higher mode effects. In addition, because of large distances between major piers or supports, large out-of-phase displacements may occur, and as a consequence analysis should be based on multiple-support seismic excitations. Accordingly, when designing rigid-frame bridges to resist earthquake forces and deformations, it is required that the natural frequencies and mode shapes of vibration be determined accurately.

In this study, a free vibration analysis of a five-span continuous rigid-frame steel bridge with V-shaped legs (see Fig. 1) is performed with three different mass matrix methods. The natural frequencies computed by the lumped, consistent, and continuous mass methods are given in tabular form, and the applicability of an approximation method is discussed. Because the structural geometry of the rigid-frame bridge shown in Fig. 1 is asymmetrical with a gentle longitudinal gradient of 2.600%, several of the natural frequencies are closely grouped and the mode shapes are complex. The Square-Root-of-Sum-of-Squares (SRSS) method and the Complete Quadratic Combination (CQC) method are applied in seismic analysis for combining modal maxima. Lastly, the results calculated by both the SRSS and CQC methods are compared with those of the time history response analysis and their applicability is investigated.

NATURAL VIBRATION ANALYSIS

From an analytical standpoint as well as an idealization of structures, it is convenient to divide the coordinate system into two different basic types as shown in Fig. 2. The first type is a distributed coordinate system [or distributed-parameter system (Refs. 1,2)], which is applied to structures whose properties are continuously distributed in space, and to problems in which the forces are distributed. In this case, the basic relation between forces and displacements for a beam segment subjected to axial and flexural vibrations is obtained by using general solutions of differential equations of motion. The above equations lead to a dynamic flexural-stiffness matrix, which is a function of the natural circular frequency of vibration. This approach results in exact solutions and is called the eigen stiffness matrix method (Refs. 3,4) or the continuous mass method (Ref. 5).

The second type of mass system to be distinguished is a discrete coordinate system [or lumped-parameter system (Refs. 2,6)], which defines forces and displacements at a set of discrete points in terms of components having specified directions. The analytical procedure for this type can be greatly simplified as an eigenvalue problem because the inertia forces are developed only at these points. In the framework structures, the lumped mass matrix (Refs. 1,4,7) is derived as a diagonal matrix by applying half the mass (and it's associated mass-moment) of each beam to the appropriate nodal point. Moreover, the mass influence coefficients are evaluated by a procedure similar to that used to determine the static stiffness coefficients. The resulting matrix is called the consistent mass matrix (Refs. 1,7), and it contains many off-diagonal terms due to the effect of mass coupling.

DYNAMIC RESPONSE ANALYSIS

In designing earthquake-resistant structures, the maximum value of the response of structures to earthquakes is the most significant quantity. The dynamic equilibrium equation for a structural system subjected to a ground acceleration $\ddot{u}(t)$ is written as follows (Ref. 8):

$$[M]\{\ddot{U}\} + [C]\{\dot{U}\} + [K]\{U\} = \{Mo\}\ddot{u}(t) \tag{1}$$

in which [M], [C], and [K] are the mass, damping, and stiffness matrices, respectively. The relative displacements, velocities, and accelerations are indicated by {U}, {$\dot{U}$}, and {$\ddot{U}$}. The column vector {Mo} contains the components of mass in the x- and y-directions. The solution {U} of Eq. (1) is found by the mode superposition

$$\{U\} = [\Phi]\{Y\} \tag{2}$$

in which [Φ] is the modal matrix, and {Y} represents the normal coordinates. By substituting Eq. (2) into Eq. (1) and premultiplying by the transpose of [Φ], Eq. (1) becomes

$$[\Phi]^T[M][\Phi]\{\ddot{Y}\} + [\Phi]^T[C][\Phi]\{\dot{Y}\} + [\Phi]^T[K][\Phi]\{Y\} = [\Phi]^T\{Mo\}\ddot{u}(t) \tag{3}$$

For proportional damping, the mode shapes have the following properties:

$$\{\Phi_i\}^T[M]\{\Phi_i\} = m_i, \quad \{\Phi_i\}^T[K]\{\Phi_i\} = \omega_i^2 m_i, \quad \{\Phi_i\}^T[C]\{\Phi_i\} = 2\zeta_i\omega_i m_i \tag{4a-c}$$

in which $\{\Phi_i\}$ is the i-th column of [Φ] representing the i-th mode shape, m_i is the i-th modal mass, ω_i is the i-th natural circular frequencies, and ζ_i is the damping ratio for mode i. Due to the orthogonal properties of the mode shapes, Eq. (3) reduces to a set of uncoupled equations in which the differential equation of motion has the same form for both the distributed coordinate system and the discrete coordinate system:

$$\ddot{Y}_i + 2\zeta_i\omega_i\dot{Y}_i + \omega_i^2 Y_i = p_i\ddot{u}(t) \tag{5}$$

and

$$p_i = \{\Phi_i\}^T\{Mo\}/m_i \tag{6}$$

in which p_i is the participation factor for mode i. The equation (5) for the i-th mode is independent of those for all other modes. Therefore, it may be integrated directly to yield the time history solution [the normal displacement $Y_i(t)$] for normal coordinates. The total structural displacements {U} are obtained from Eq. (2).

To evaluate the earthquake response of Multi-Degree-of-Freedom (MDOF) systems at any time, t, involves the computation of the Duhamel integral at that time for each significant response mode. Hence, the evaluation of the maximum response (displacements and forces) requires that each modal response be computed in this way for each time during the earthquake history. This obviously constitutes a major computation effort and makes an approximate analysis based on the ground-motion response spectra an attractive alternative. A number of different formulas have been proposed to obtain a more reasonable estimate of the maximum response from the spectral values. The simplest and most popular of these is the Square-Root-of-Sum-of-Squares (SRSS) method; the maximum displacement response of each mode is given below (Refs. 1,9):

$$U_{i,max} = \sqrt{\sum_j (\Phi_{ij} Y_{j,max})^2} \tag{7}$$

in which $Y_{j,max}$ is the maximum response of each mode.

On the other hand, the Complete Quadratic Combination (CQC) method requires that all modal response terms be combined by the application of the following equation (Ref. 8): For a typical displacement, u_k

$$u_k = \sqrt{\sum_i \sum_j u_{ki}\rho_{ij}u_{jk}} \tag{8}$$

in which u_{ki} is a typical component of the modal displacement response vector. In general, the cross-modal coefficients ρ_{ij} are functions of the duration and frequency content of the loading and of the natural frequencies and damping ratios of the structure. If the duration of the earthquake is long compared to the periods of the structure, and if the earthquake spectrum is smooth over a wide range of frequencies (for a white-noise input), it is possible to approximate the coefficients by the following (Refs. 8,10):

$$\rho_{ij} = \frac{8\sqrt{(\zeta_i\zeta_j)}(\zeta_i + r\zeta_j)r^{3/2}}{(1-r^2)^2 + 4\zeta_i\zeta_j r(1+r^2) + 4(\zeta_i^2+\zeta_j^2)r^2} \tag{9}$$

in which $r = \omega_j/\omega_i$. For constant modal damping ζ this equation reduces to

$$\rho_{ij} = \frac{8\zeta^2(1+r)r^{3/2}}{(1-r^2)^2 + 4\zeta^2 r(1+r)^2} \tag{10}$$

If the cross-modal coefficients ρ_{ij} of all natural modes are $\rho_{ij}=1$ for i=j and $\rho_{ij}=0$ for $i\neq j$, then the maximum response of displacements calculated by the CQC method agrees with that by the SRSS method.

NUMERICAL RESULTS

Numerical Example A numerical example is presented to demonstrate the effectiveness of the analytical method described here and to investigate some dynamic characteristics of vertically vibrating rigid-frame bridges. The computations were based on data from the Shibechari Bridge located in Hokkaido, Japan. The bridge geometry and the span lengths are given in Fig. 1. The boundary conditions consist of a pin support at A1, fixed supports at P1 and P2, and a roller support at A2. Figures 3 and 4 are the longitudinal and vertical ground motion records of the South Hidaka earthquake taken at Horoman on January 21, 1970, respectively. This earthquake is a record taken approximately 25 Km from the

epicenter of a strong earthquake of M=6.7. The maximum accelerations of longitudinal and vertical ground motions are 174.14 gal and 88.29 gal, respectively.

Natural Frequencies The natural circular frequencies computed by the lumped, consistent, and continuous mass methods, corresponding to the first 20 modes of the numerical example, are presented in Table 1: The number of beam segments is N = 80. In general, the values of the natural circular frequencies obtained by using the lumped mass method are small in comparison with those of the exact solutions calculated with the continuous mass method. In contrast, the values of the natural circular frequencies resulting from the consistent mass method are relatively large. Figure 5 shows the relationship between the natural circular frequency ratio ω/ω^* and the order of natural modes for the numerical example of the five-span continuous rigid-frame bridge with V-shaped legs. Here ω^* is the exact solution obtained by the continuous mass method, and ω is the approximate solution obtained by using the lumped and consistent mass methods. It is seen that the natural circular frequencies calculated by both the lumped and the consistent mass methods gradually approach the exact solutions as the number of beam segments, N, increases. The natural circular frequencies calculated by the use of the lumped and consistent mass methods are the lower and upper bounds to the exact solutions, respectively. It may be also pointed out that for the same number of beam segments, the use of the consistent mass method provides eigenvalues of greater accurate than does the lumped mass method.

The mathematical relationship among the lumped, consistent, and continuous mass methods is established in Refs. 4 and 7. The power series expansion of the eigen stiffness matrices $[K_{ae}]$ and $[K_{fe}]$ under axial and flexural vibrations in the vertical plane may be written in matrix notation as follows:

$$[K_{ae}] = [K_a] - [M_{a1}]\omega^2 - [M_{a2}]\omega^4 \cdot \cdot \cdot \cdot \cdot \quad (11a)$$

$$[K_{fe}[= [K_f] - [M_{f1}]\omega^2 - [M_{f2}]\omega^4 \cdot \cdot \cdot \cdot \cdot \quad (11b)$$

In the case of longitudinal vibrations, the stiffness matrix $[K_a]$ and the first order mass matrix $[M_{a1}]$ agree precisely with the static stiffness matrix and the consistent mass matrix, respectively, for axial vibration in the discrete coordinate system. Also, the square matrices $[K_f]$ and $[M_{f1}]$ of Eq. (11b) for lateral vibrations agree precisely with the static-stiffness and mass-influence coefficients evaluated by using the cubic Hermitian polynomials as the interpolation functions, respectively. It is concluded, therefore, that the consistent mass method is equivalent to a special case of the continuous mass method obtained by neglecting terms of higher than second order. Moreover, it is estimated that the lumped mass method is a truncated result of the consistent mass method obtained by omitting the mass coupling. The relationship between the exact and approximate methods is clearly demonstrated by the above mathematical derivations, and is also easily comprehensible from the computed results shown in Fig. 5.

Maximum Response of Displacements By assuming 2 percent damping and the natural frequencies obtained by the consistent mass method, the participation factors p_i of Eq. (6) and the modal cross-correlation coefficients ρ_{ij} of Eq. (10) can be calculated as shown in Table 2. As seen in the example structure, the values of the participation factors in the higher modes of vibration are large in comparison to those in the first few modes. The participation factors in the 6th and 7th modes exhibit especially large values. The closeness of the natural frequencies between the 9th and 10th modes and between 11th and 12th modes is recognized; also, the modal cross-correlation coefficients corresponding to these modes are very large in comparison with the others in Table 2. Therefore, it can be considered for this case that the higher modes significantly influence seismic analysis for combining modal maxima.

The response values for horizontal displacement x (cm) and vertical displacement y (cm) calculated by the SRSS method and the CQC method are shown in Table 3.

Also, the numerical results of the time history response analysis, in which all 20 modes were used, are presented in comparison with two conventional methods of combining modal maxima. It is clear that the SRSS method greatly underestimates the horizontal displacements in the direction of the motion. Also, the vertical displacements found by the CQC method are underestimated. In general, the calculated results of the time history response analysis are higher than those of both the SRSS method and the CQC method. However, there is no considerable difference between the SRSS method and the CQC method in response spectrum calculations of the five-span continuous rigid-frame bridge with V-shaped legs.

CONCLUSIONS

The mathematical relation between the exact method based on the general solutions of differential equations of motion and the approximate method based on a finite element approach is established in this presentation. The values of natural frequencies calculated by using the lumped and consistent mass methods are the lower and upper bounds, respectively, to the exact solutions. Assuming the same number of beam segments, the eigenvalues of rigid-frame bridges can be calculated more accurately by the consistent mass method than by the lumped mass method.

In the response spectrum calculations, the values of participation factors and the modal cross-correlation coefficients estimated by some higher modes are larger than those estimated by the first few lower modes. For two-dimensional rigid-frame bridge structures, it is proposed that the SRSS method and the CQC method of combining modal maxima yield good results when compared to time history response calculations. This study provides a basis for future theoretical research and may be applied to the structural dynamics of thin-walled three-dimensional structures with inclusion of warping effects.

REFERENCES

1. Clough, R, W., and Penzien, J., Dynamics of Structures, McGraw-Hill Book Co., (1975).
2. Jacobsen, L. S., and Ayre, R. S., Engineering Vibrations, McGraw-Hill Book Co., (1958).
3. Hayashikawa, T., and Watanabe, N., "Dynamic Behavior of Continuous Beams with Moving Loads," Journal of Engineering Mechanics Division, Proc. of ASCE, Vol. 107, No. EM1, Feb., pp. 229-246, (1981).
4. Hayashikawa, T., and Watanabe, N., "Free Vibration Analysis of Continuous Beams," Journal of Engineering Mechanics, Proc. of ASCE, Vol. 111, No. 5, May, pp. 639-652, (1985).
5. Ovunc, B. A., "Dynamics of Frameworks by Continuous Mass Method," Journal of Computers and Structures, Vol. 4, pp. 1061-1089, (1974).
6. Hurty, W. C., and Rubinstein, M. F., Dynamics of Structures, Prentice-Hall, Inc., (1964).
7. Paz, M., Structural Dynamics: Theory and Computation, Van Nostrand Reinhold Company, (1980).
8. Wilson, E. L., Kiureghian, A. D., and Bayo, E. P., "A Replacement for the SRSS Method in Seismic Analysis, Earthquake Engineering and Structural Dynamics, Vol. 9, pp. 187-194, (1981).
9. Okamoto, S., Introduction to Earthquake Engineering, Second Edition, University of Tokyo Press, (1984).
10. Kiureghian, A. D., "On Response of Structures to Stationary Excitation," Earthquake Engineering Research Center, University of California, Berkeley, Report No. UCB/EERC-79/32, (1979).

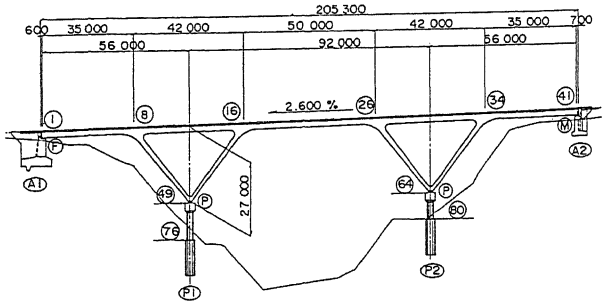

Fig. 1 General View of Rigid-Frame Bridge

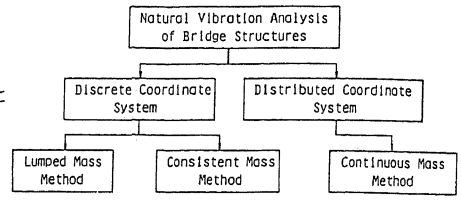

Fig. 2 Schematical Description

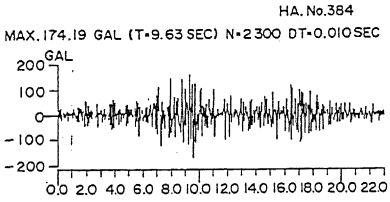

Fig. 3 Longitudinal Ground Motion

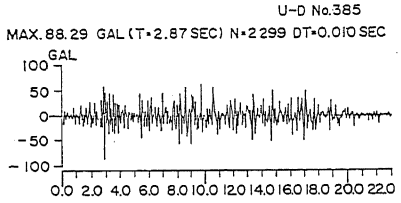

Fig. 4 Vertical Ground Motion

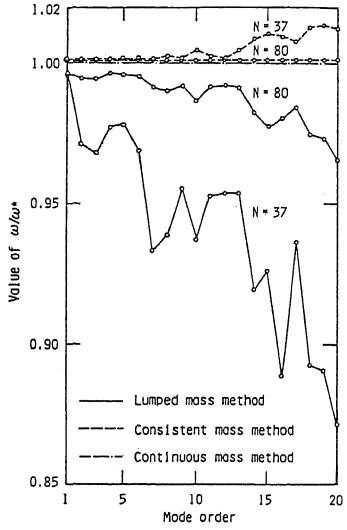

Fig. 5 Comparison of Natural Circular Frequencies

Table 1 Natural Circular Frequencies Computed by Three Different Mass Methods

Mode order	Lumped mass method	Consistent mass method	Continuous mass method
1	12.0779	12.1343	12.1280
2	15.9130	16.0086	16.0000
3	16.9244	17.0312	17.0220
4	19.5263	19.6058	19.5950
5	23.1490	23.2537	23.2406
6	25.5647	25.6921	25.6773
7	29.6828	29.9651	29.9478
8	36.1952	36.5749	36.5529
9	41.0448	41.3972	41.3728
10	41.7743	42.3727	42.3452
11	45.6868	46.1153	46.0867
12	46.1368	46.5411	46.5132
13	48.4642	48.9259	48.8953
14	61.8550	63.0179	62.9664
15	63.0435	64.5331	64.4789
16	68.3102	69.7503	69.6821
17	69.2541	70.4185	70.3531
18	80.5942	82.7604	82.6762
19	88.1759	90.7033	90.6014
20	91.8246	95.2146	95.1020

Table 2 Modal Cross-Correlation Coefficients

Mode order	Natural frequency (Hz)	Participation factor P_i	Modal cross-correlation coefficients ρ_{ij}											
			1	2	3	4	5	6	7	8	9	10	11	12
1	1.931	2.119	1.0000	0.0200	0.0134	0.0066	0.0035	0.0025	0.0016	0.0010	0.0008	0.0007	0.0006	0.0006
2	2.548	1.491	0.0200	1.0000	0.2940	0.0372	0.0110	0.0068	0.0037	0.0023	0.0015	0.0014	0.0011	0.0011
3	2.711	-2.847	0.0134	0.2940	1.0000	0.0744	0.0159	0.0091	0.0047	0.0024	0.0017	0.0016	0.0013	0.0013
4	3.120	-3.345	0.0066	0.0372	0.0744	1.0000	0.0518	0.0211	0.0085	0.0038	0.0025	0.0024	0.0019	0.0018
5	3.701	1.113	0.0035	0.0110	0.0159	0.0518	1.0000	0.1383	0.0240	0.0074	0.0045	0.0041	0.0031	0.0030
6	4.089	12.293	0.0025	0.0068	0.0091	0.0211	0.1383	1.0000	0.0630	0.0123	0.0067	0.0060	0.0043	0.0042
7	4.769	6.301	0.0016	0.0037	0.0047	0.0085	0.0240	0.0630	1.0000	0.0384	0.0148	0.0128	0.0082	0.0079
8	5.821	-2.995	0.0010	0.0023	0.0024	0.0038	0.0074	0.0123	0.0384	1.0000	0.0942	0.0685	0.0286	0.0265
9	6.589	0.752	0.0008	0.0015	0.0017	0.0025	0.0045	0.0067	0.0148	0.0942	1.0000	0.7468	0.1205	0.1042
10	6.744	3.758	0.0007	0.0014	0.0016	0.0024	0.0041	0.0060	0.0128	0.0685	0.7468	1.0000	0.1823	0.1535
11	7.339	-1.972	0.0006	0.0011	0.0013	0.0019	0.0031	0.0043	0.0082	0.0286	0.1205	0.1823	1.0000	0.9498
12	7.407	1.612	0.0006	0.0011	0.0013	0.0018	0.0030	0.0042	0.0079	0.0265	0.1042	0.1535	0.9498	1.0000

Table 3 Comparison of Modal Combination Methods

Analytical method	Horizontal displacements X (cm)			Vertical displacements Y (cm)		
	point 11	point 21	point 46	point 11	point 21	point 46
SRSS method	2.46	4.44	13.13	15.69	11.88	11.12
CQC method	2.69	4.86	12.37	15.02	11.53	10.23
Time history response analysis	3.26	6.00	14.45	23.65	14.96	12.76